Three-dimensional finite element analysis of maxillary protraction with labiolingual arches and implants

Chang Liu,[a] Xianchun Zhu,[b] and Xing Zhang[c]
Changchun, Jilin, China

Introduction: In this study, we aimed to evaluate the effects of maxillary protraction using traditional labiolingual arches and implant-type protraction devices before orthopedic treatment of patients with skeletal Class III malocclusion. **Methods:** A 3-dimensional finite element model of the maxillofacial bones with high biologic similarity and including the sutures was constructed. Through stress and displacement calculations, a biomechanical study was performed for the maxillofacial bones, mandible, and sutures. **Results:** We quantified detailed changes in the sutures with 2 protraction methods to analyze their effects on the growth of the maxillofacial bones. **Conclusions:** (1) The labiolingual arch is suitable for skeletal Class III patients with crossbite and deep overbite. The frontomaxillary and zygomaticomaxillary sutures played major roles in the forward displacement and counterclockwise rotation of the maxilla. The temporozygomatic and pterygopalatine sutures did not change significantly. (2) The implant type of protraction device is suitable for skeletal Class III patients with crossbite and open bite. Both the frontomaxillary and zygomaticomaxillary sutures played decisive roles in the forward displacement and clockwise rotation of maxilla. The temporozygomatic and pterygopalatine sutures showed small changes. (3) The labiolingual arch caused less stimulatory growth on the maxilla, whereas the implant caused greater stimulatory growth on the maxilla. Protraction with the labiolingual arch is more suitable for early skeletal Class III patients at a younger age; protraction with an implant is applicable to skeletal Class III patients in the late mixed dentition or early permanent dentition. (Am J Orthod Dentofacial Orthop 2015;148:466-78)

Skeletal Class III malocclusion is a common dental abnormality. This problem, which is primarily caused by the insufficient development of the maxillary bone, tends to worsen with age.[1-3] Applying maxillary protraction can effectively direct the maxillary bone to grow forward, and the effect of this procedure has been widely acknowledged.[4-8] Among traditional protraction devices, the labiolingual arch has a superior effect.[8-10] However, when this appliance guides the maxillary bone to grow forward, the maxillary anterior teeth also inevitably incline to the lip side: ie, the dental effects become stronger than or equal to the bone effects. The labiolingual arch is applied in the orthopedic treatment of crossbite accompanied by a deep overbite occlusion.[2] For skeletal Class III malocclusion patients with an open-bite tendency, the maxillary bone should be rotated clockwise during orthodontic treatment; the bone effects should be stronger than the dental effects. This condition cannot be achieved using traditional protraction devices. Moreover, applying an implant type of protraction appliance can solve these problems. Based on the study of Smalley et al,[11] the bone effects of maxillary protraction with implants should be significantly stronger than the dental effects.

To evaluate traditional maxillary protraction and implant-type protraction devices from the perspective of biomechanics, as well as to provide clinical treatment guidelines, in this study we first constructed a 3-dimensional (3D) finite element model of the maxillofacial bones with high biologic similarity and including the sutures. The model was designed to simulate

[a]Assistant professor, Changchun Stomatological Hospital; assistant professor, School of Stomatology, Jilin University, Changchun, Jilin, China.
[b]Associate professor, School of Stomatology, Jilin University, Changchun, Jilin, China.
[c]Associate professor, Changchun Institute of Optics, Fine Mechanics and Physics, Chinese Academy of Sciences, Changchun, Jilin, China.
All authors have completed and submitted the ICMJE Form for Disclosure of Potential Conflicts of Interest, and none were reported.
Supported by the National Natural Science Foundation of China (grant number 61204056).
Address correspondence to: Xianchun Zhu, Jilin University, School of Stomatology, No. 3888 Dongnanhu Road, Changchun, Jilin, China; e-mail, zx3930@sina.com.
Submitted, July 2014; revised and accepted, April 2015.
0889-5406/$36.00

http://dx.doi.org/10.1016/j.ajodo.2015.04.028

labiolingual arch loading and implant-type maxillary protraction appliances. Second, stress and displacement values were obtained through calculations. Third, a biomechanical study was performed for the sutures, the maxillofacial bones, and the mandible. We quantified the detailed changes in the sutures with 2 protraction methods to analyze the effects of these methods on the growth of the maxillofacial bone, particularly on the 4 sutures that are closely related to the growth of these bones. Finally, an in-depth discussion is provided based on our results.

MATERIAL AND METHODS

This study was approved by the medical ethics committee of the Hospital of Stomatology, Jilin University, in China.

First, we established a 3D finite element model of the maxillofacial bones with a physical model of the sutures. A 16-year-old Asian volunteer with normal occlusion, good periodontal health, and no temporomandibular joint (TMJ) disease was chosen to be the model.

The volunteer's craniofacial complex was consecutively scanned in multislices in the normal way. In the process of scanning, the volunteer was required to lie on her back with her chin lifted, her head fixed, and her mouth open slightly, and bite a premade 2-mm-thick plastic piece to keep the teeth apart. Her bite plane was identified, and the scanned slice was parallelized with the bite plane. Scan parameters were tube voltage, 120 kV; electric current, 250 mA; bed speed, 0.8 seconds per circle; slice thickness, 0.67 mm; and interval, 0.33 mm. We obtained 456 images by cleaning up the computed tomography (CT) DICOM data from the scans and recorded them on compact disks.

The CT data output in BMP format was transferred to Mimics software (version 10.0; Materialise, Leuven, Belgium), a medical visualization software and a rectangular coordinate system with the x-, y-, and z-axes built up according to slice image data from the CT scans (x-axis indicates axial; y-axis, sagittal; z-axis, coronal). For each slice's CT image, its outline map was formed into a closed outline curve. Then, based on the 0.33-mm interval between CT slices, each outline that represented a CT scan slice was transferred to its position according to its z-value, and a rough 3D model of the maxillofacial bones was automatically built using the 3D modeling function of the Mimics software (Fig 1). Based on this model, a new 3D finite element model of the maxillofacial bones was generated after deleting the unnecessary skull part, removing the constructed defects between the teeth, separating the maxillary and mandibular dentitions, and smoothing the surface. The

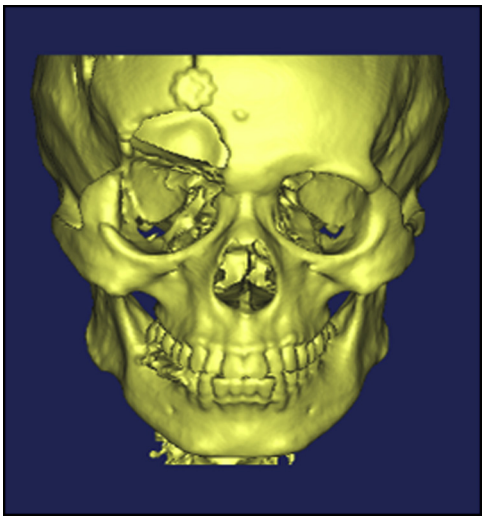

Fig 1. Preliminary 3D model of the maxillofacial bones built by the Mimics software after the CT scan.

right orbital rim of this model had some defects caused by low and irregular bone density; these defects were fixed during the finite element modeling.

The 3D STL model built was imported to software (Geomagic, Rock Hill, SC), a professional reverse-engineering software. An incision on the maxillofacial bones was determined by Boolean calculation along the track of the sutures on it, and the basic NURBAS (Non-Uniform Rational B-Splines) surface model which is necessary to the analysis was obtained.

Surface element data that were corrected in Geomagic were imported to ICEM CFD software (ANSYS, Canonsburg, Pa) at the same time that the surfaces corresponding to the frontomaxillary, zygomaticomaxillary, temporozygomatic, and pterygopalatine sutures were built up on the model of the maxillofacial bones, and filling elements were divided according to surface of model on the basis of the octree element technique.

On the basis of an initially formed tetrahedron net, a 1-mm-thick prismatic net was formed through the projections of the frontomaxillary, temporozygomatic, and pterygopalatine suture trends on the characteristic face; thus, a 3D finite element model with solid models of the sutures was formed. We selected the grids of corresponding faces at the malomaxillary suture and generated a zygomaticomaxillary suture grid in the direction of a normal vector.

Finally, we obtained a 3D finite element model of the maxillofacial bones with 86757 nodes and 485915 cubes, including a physical model of the frontomaxillary, zygomaticomaxillary, temporozygomatic, and pterygopalatine sutures (*blue lines* in Fig 2). We imported the

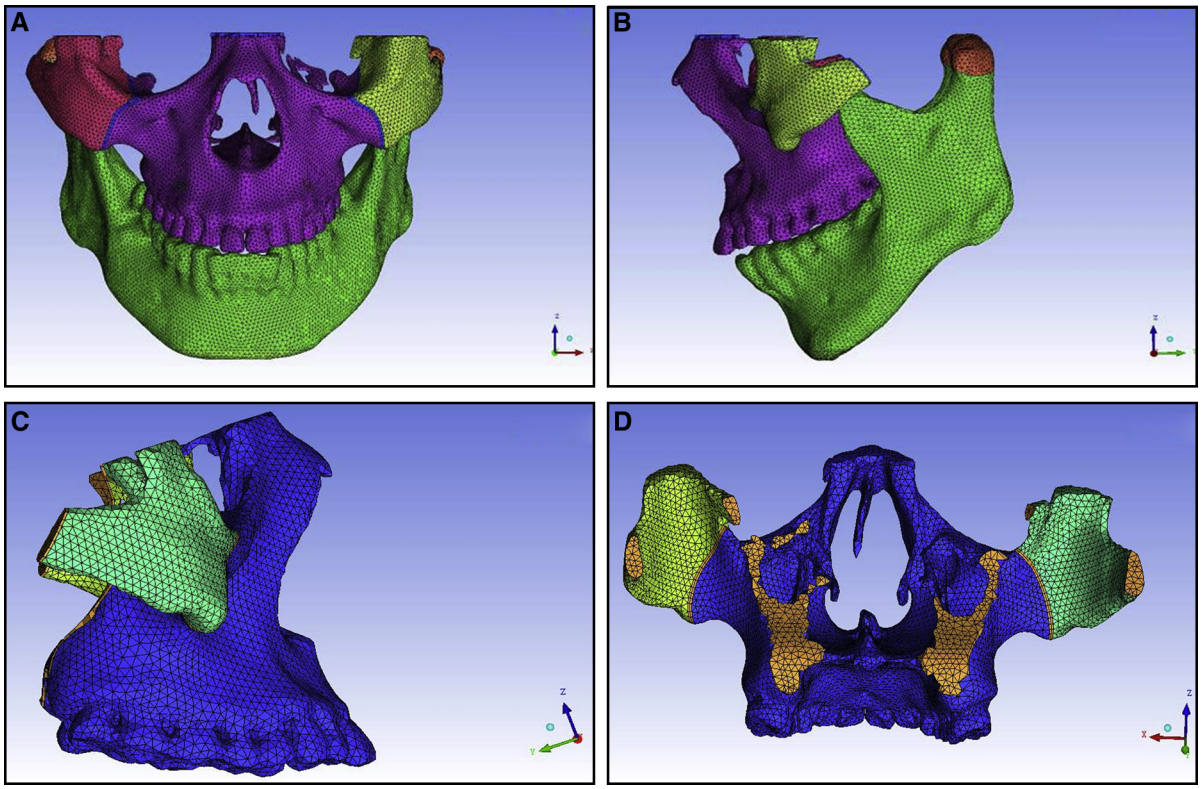

Fig 2. Three-dimensional finite element model of the maxillofacial bones with the physical models of the sutures: **A,** frontomaxillary and zygomaticomaxillary sutures; **B,** temporozygomatic suture; **C,** lateral view of the pterygopalatine suture; **D,** back view of the pterygopalatine suture.

Table I. Elastic modulus and Poisson's ratio[4]

Part	*Modulus of elasticity (MPa)*	*Poisson's ratio*
Bones	1.37×10^4	0.30
Teeth	2.07×10^4	0.30
Sutures	38.6	0.45

repaired STL into the ICEM CFD software for meshing and assigned values to the material properties according to the final geometric structure. Table I shows the assignments of the modulus of elasticity and Poisson's ratio.

The principle of the design of an intraoral device for labiolingual arch protraction is to connect the entire maxillary dental arch into a whole to reduce the tooth effect. According to this, the model was simplified without cutting the maxillary teeth to simulate the intraoral device using a labiolingual arch. The protraction mask was connected directly to the chin to simulate the chin support. Finally, a 3D finite element model of the maxillofacial region with the intraoral device for labiolingual arch protraction was established (Fig 3).

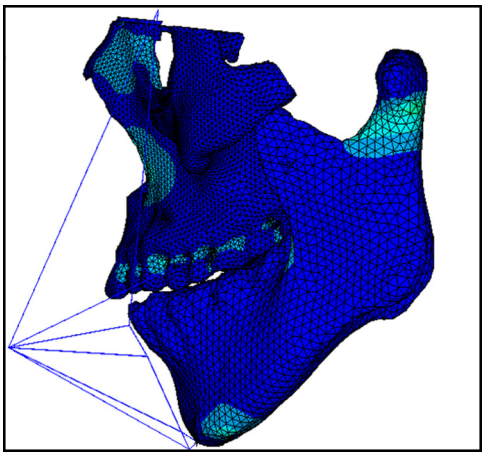

Fig 3. Maxillofacial model combined with the labiolingual arch maxillary protraction appliance.

The protraction model with the implant was simplified by applying the point between the root apices of both maxillary canines and first premolars as the traction

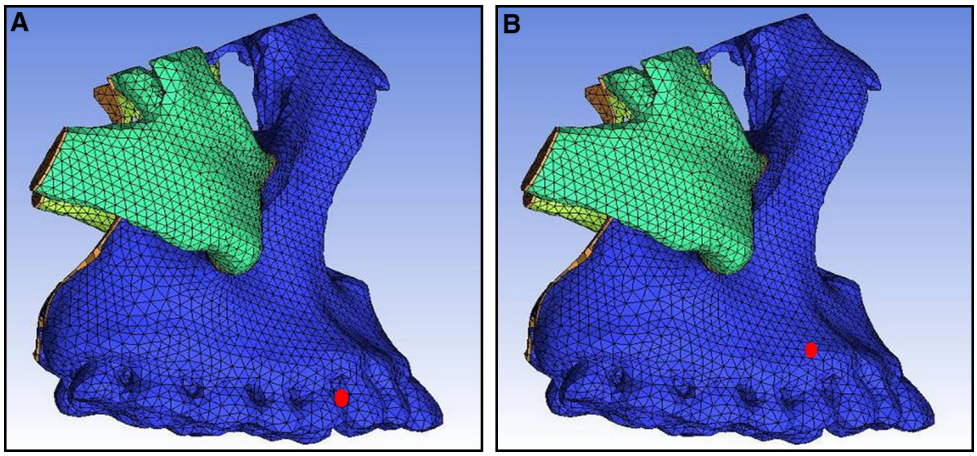

Fig 4. Illustration of the action point (*red dot*) of **A,** labiolingual arch protraction, and **B,** protraction with implant.

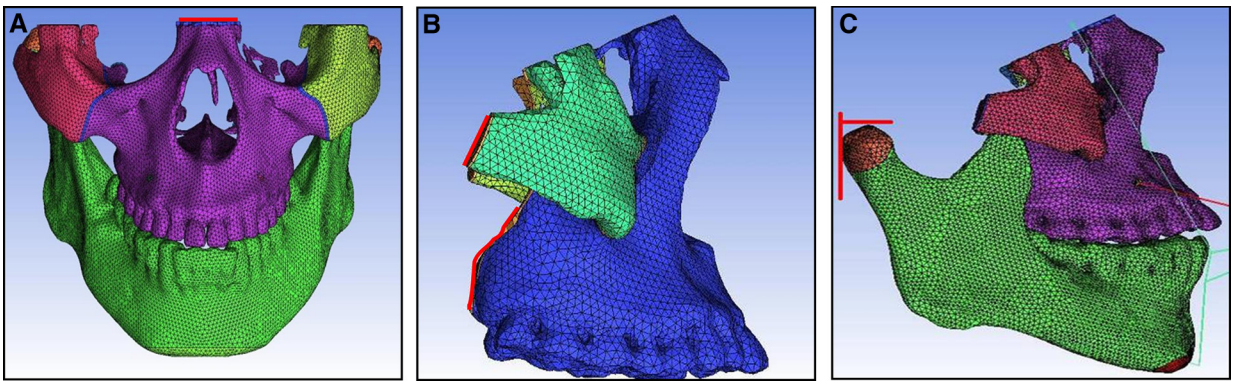

Fig 5. Boundary constraints represented by *red lines*: **A,** frontomaxillary suture; **B,** malomaxillary suture; **C,** condylar process.

point. The model of the extraoral protraction mask previously described was used (Fig 3).

In the labiolingual arch protraction model, the maxillary arch was considered as a whole, and the action point of protraction was set between the maxillary canine and the first premolar (Fig 4, *A*). In the protraction model with the implant, the action point was set between the root apices of both maxillary canines and first premolars (Fig 4, *B*); ie, the implant achieved 100% osseointegration with the maxillary bone. The materials used in protraction were spring units; the other extraoral protraction mask was made of rigid materials. According to the lever principle, the reaction force generated by protraction was mostly transmitted to the mandible through the mask.

The growth of the maxilla is mainly accomplished through bone deposition at the frontomaxillary, zygomaticomaxillary, temporozygomatic, and pterygopalatine sutures. Except for the zygomaticomaxillary suture, the other 3 sutures are all located on the edges of the maxillofacial bones. Therefore, the boundary constraints with zero displacement and zero rotation were applied on the tangent lines of the outer margins of the frontomaxillary, temporozygomatic, and pterygopalatine sutures (Fig 5). The mandible was included in the model. The TMJ connection between the mandible and the maxilla was set as absent. Two tangent lines from condylion and the protrusion of the outer margin of the condylar process were made, respectively. The boundary constraints with zero displacement and zero rotation were applied on the 2 tangent lines.

In the labiolingual arch protraction model, the action point was set at adjacent points of both maxillary canines and first premolars to simulate the position of the protraction hook. In the protraction model with the implant, the action point was set

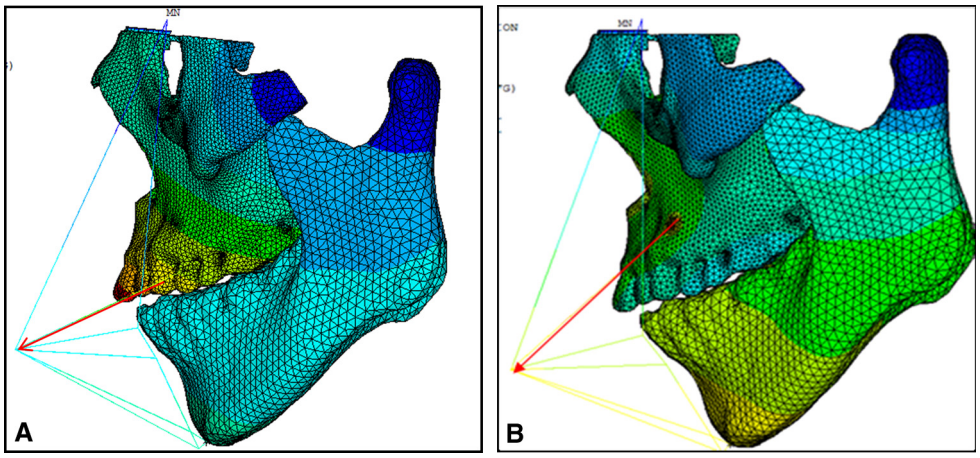

Fig 6. Direction of protraction (*red arrow*): **A,** labiolingual arch protraction; **B,** protraction with implant.

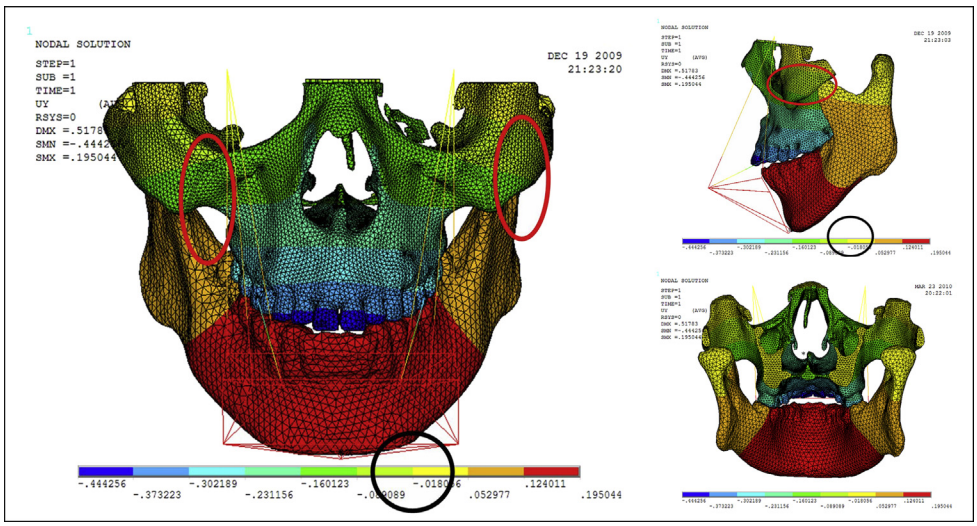

Fig 7. Displacement nephogram along the y-axis after loading of the labiolingual arch protraction model.

between the root apices of both maxillary canines and first premolars to simulate the implant. In both methods, 800 g of protraction force was applied on both sides at a 20° to 30° angle with respect to the occlusal plane, depending on the position of the lower lip (Fig 6).

RESULTS

Displacement nephograms along the y-axis and z-axis after loading of the protraction model using the labiolingual arch and the implant are shown in Figures 7-10. The x-axis representing the horizontal displacement, which was not the displacement considered in protraction, was ignored.

The forward direction of the y-axis indicates a negative value, and the backward direction of the y-axis indicates a positive value; the upward direction of the z-axis indicates a positive value, and the downward direction of the z-axis indicates a negative value. The displacement distributions along the y-axis and z-axis were obtained by the data extraction function of the ANSYS software (Table II).

Stress distribution nephograms of the maxilla in the protraction modes using the labiolingual arch and the implant were calculated (Fig 11). The 4 sutures were extracted to obtain the stress distribution nephograms (Fig 12). As shown in Table III, the suture stress distributions of the 2 types of protraction were statistically analyzed and compared.

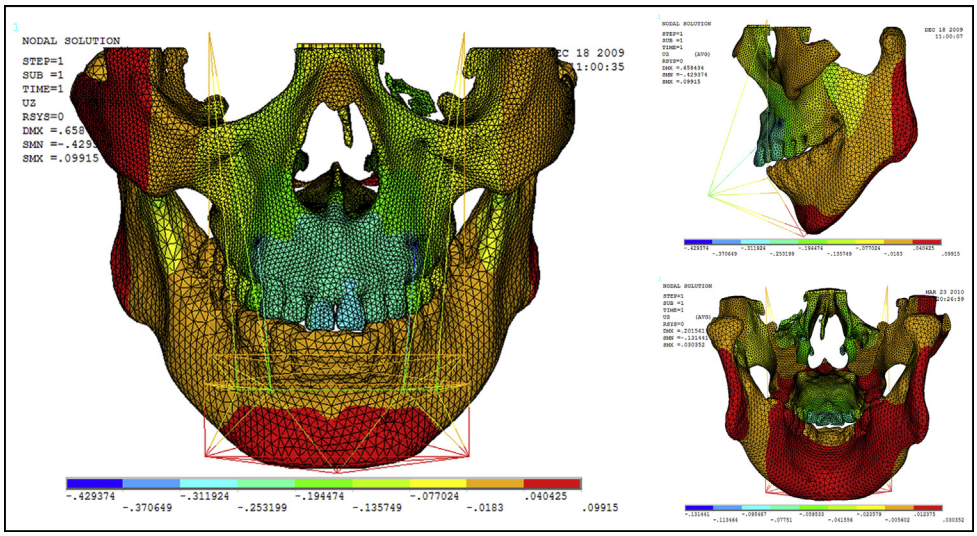

Fig 8. Displacement nephogram along the y-axis after loading of the protraction model with an implant.

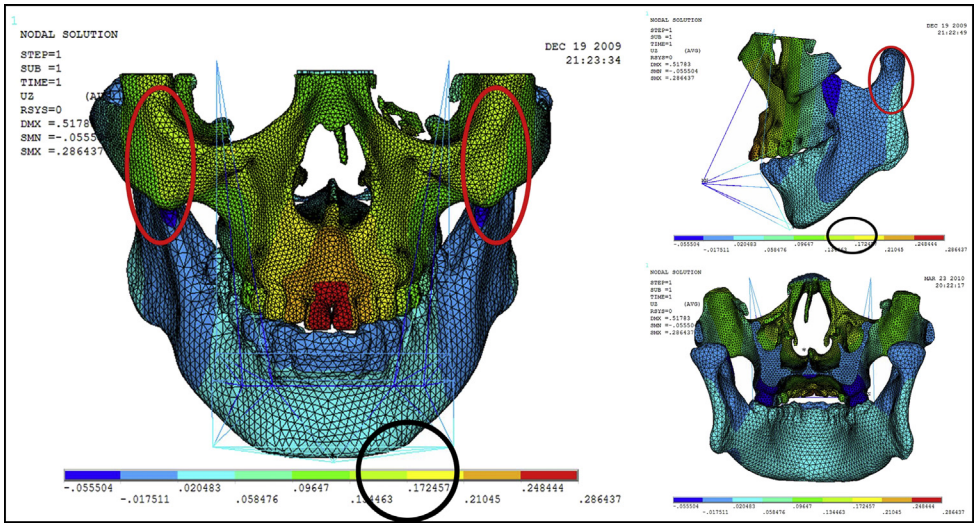

Fig 9. Displacement nephogram along the z-axis after loading of the labiolingual arch protraction model.

DISCUSSION

During previous 3D finite element modeling studies of the maxillofacial bones, the whole maxillary complex was always supposed to be continuous, homogeneous, and isotropic without suture grids.[12-15] Thus, in the sutures, stress was presented as homogeneous, and there would be a large error once the model was loaded.

"Suture" generally refers to the cells and fibrous tissues located between the craniofacial bone and the opposite bone edge, as well as those surrounding the bone edge. A suture is formed by the interactions between osteoblasts and fibroblasts. Osteoblasts and fibroblasts perform different functions. Osteoblasts secrete collagen and other specialized proteins that constitute a bone matrix. Fibroblasts inhibit the extensive proliferation of osteoblasts, thereby preventing suture formation.[16]

Several researchers have investigated factors affecting sutures. For example, Iseri et al[17] studied the maxillary palatal raphe using a finite element method and found that this structure is unconnected; thus, they did not consider the properties of suture materials. Verrue et al[18] used a 3D finite element method and constructed a dog's craniofacial bone with 18 sutures. Using this model, they hypothesized that the elastic modulus is

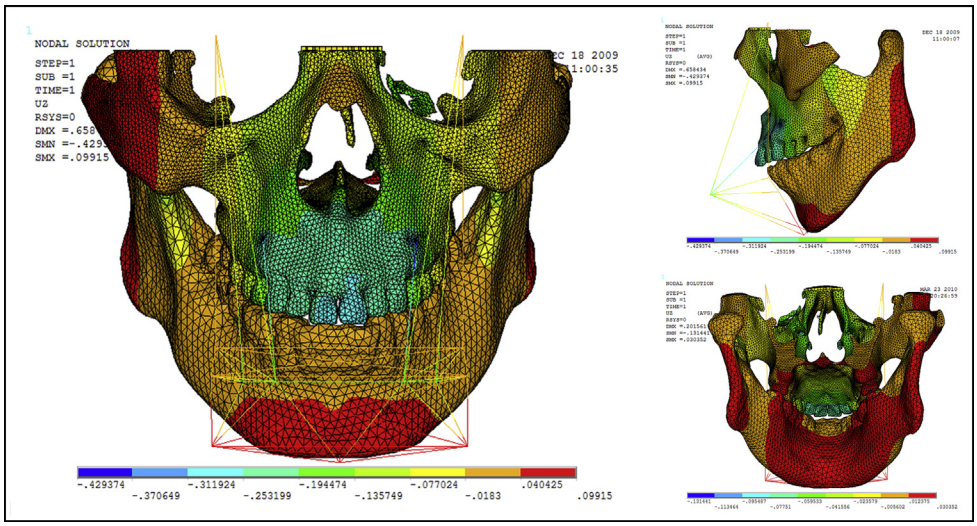

Fig 10. Displacement nephogram along the z-axis after loading of the protraction model with an implant.

Table II. Displacement distribution along y-axis and z-axis (mm)

	Displacement along y-axis		*Displacement along z-axis*	
Part	*Labiolingual arch*	*Implant*	*Labiolingual arch*	*Implant*
U1 point in the incisal edge of maxillary central incisor	−0.444	−0.163	0.249	−0.312
A-point of maxilla	−0.302	−0.275	0.210	−0.253
L1 point in the incisal edge of mandibular central incisor	0.124	0.395	−0.018	−0.018
Pogonion of mandible	0.124	0.395	0.205	0.040
Frontomaxillary suture	−0.160	−0.164	0.205	−0.077
Malomaxillary suture	−0.160	−0.275	0.134	−0.018
Temporozygomatic suture	−0.018	−0.164	−0.018	−0.018
Pterygopalatine suture	−0.018	−0.052	−0.018	−0.018

U, upper jaw; *L*, lower jaw.

probably 6850 N per square millimeter (about half of the cortical bone). Verrue et al also showed that maxillary displacement is possibly close to the result obtained by laser interferometry if the elastic modulus is approximately 1 N per square millimeter. Thus, the elastic modulus of a maxillary suture is preliminarily considered as 1 N per square millimeter. However, this result does not accurately indicate the biomechanical changes in the craniofacial complex. On the basis of these results, Verrue et al concluded that the establishment of a suture is more important than the precision of grid division in traction research.

The growth of a suture from various components is similar to that of a periodontal membrane. This similar growth pattern is possibly attributed to the components of these 2 parts. For instance, the suture is mainly composed of bone cells, fibrous cells, fibers, and blood vessels. The periodontal membrane consists of cells, matrices, fibers, and partial vessels. Furthermore, a suture exhibits biomechanical behaviors similar to those of a periodontal membrane when these parts are subjected to external forces.[19,20] For example, tension can induce bone cells to proliferate, to grow rapidly, and to form new bones.[21] Pressure can cause degenerative changes and bone absorption, thereby inhibiting bone growth.[22] On the basis of these observations, we assigned the elastic modulus of the suture as 38.6 MPa, which is similar to that of the periodontium.[19] Poisson's ratio of a suture was set at 0.45 after previous craniofacial finite element studies were comparatively analyzed.[23,24] This value is approximately equal to the actual Poisson's ratio of a suture. Additionally, loading executed on the ground of this model can have a more real stress distribution in the suture, have better maxillary influence, and provide more accurate data to clinical work. In this study, the thickness of the sutures was supposed to be 1 mm, which would not affect the accuracy of calculations but would ensure the grid quality.

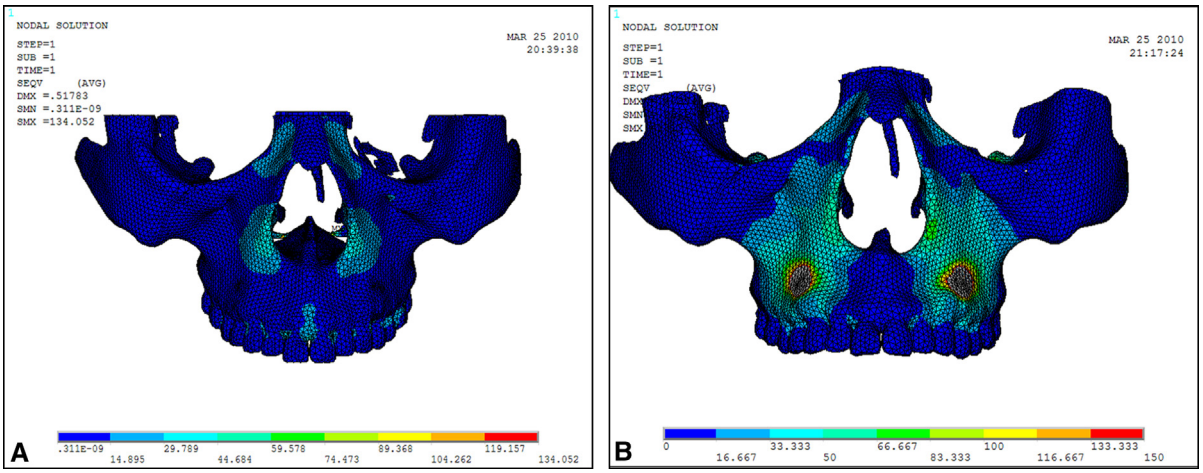

Fig 11. Stress distribution nephograms of the maxilla in the protraction models with **A,** labiolingual arch, and **B,** implant.

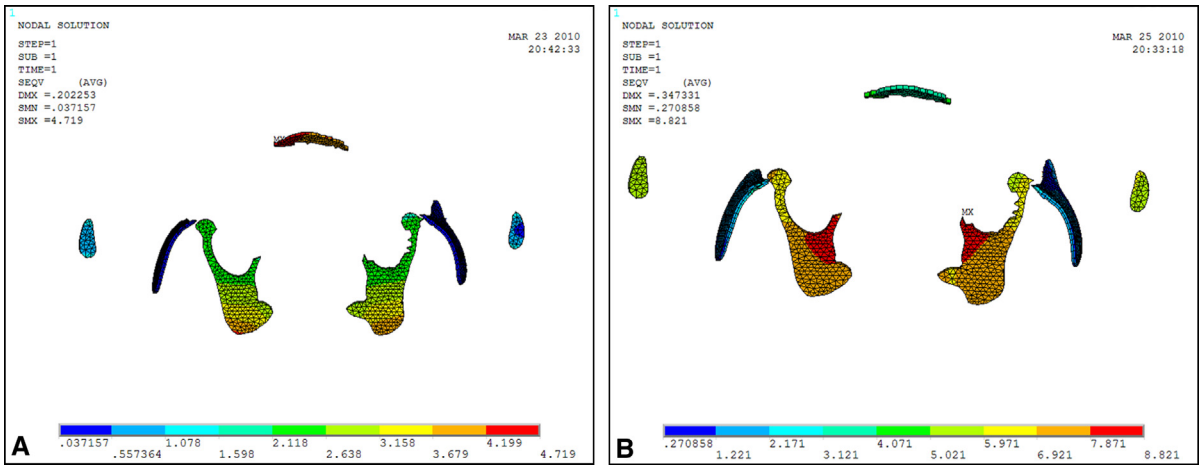

Fig 12. Stress distribution nephograms in the 4 sutures: **A,** labiolingual arch, and **B,** implant.

According to Ngan et al,[25] Cozzani,[26] Hickham,[27] Itoh et al,[28] Hata et al,[29] Billiet et al,[30] and da Silva Filho et al,[5] the protraction force should be 600 to 800 g to produce an effect. Otherwise, it may move the maxillary teeth mesially. Zeng[31] suggested that the protraction force should be at least 500 to 800 g per side, with the device worn less than 12 to 14 hours a day. Gautam et al[32] biomechanically evaluated 2 treatment modalities—maxillary protraction alone and in combination with maxillary expansion—by comparing the displacement of various craniofacial structures using the finite element method. In the first model, 1 kg of force was directed anteriorly and 30° downward relative to the occlusal plane near the canine to simulate orthopedic maxillary protraction forces.

In the labiolingual arch protraction model, the action point was set at adjacent points of both maxillary canines and first premolars to simulate the position of the protraction hook. In the protraction model with an implant, the action point was set between the root apices of both maxillary canines and first premolars to simulate the implant. For the implant type of protraction device, the miniplate was implanted into the surface of the alveolar bone, and the protraction force was increased to 500 to 1000 g. A traditional labiolingual arch protraction device is 1 type of tooth-anchored maxillary protraction, and the force is usually set to less than 500 g in clinics.[4] However, to compare the variations of maxillary bones and sutures in these protractions, the force of protraction was set to be the same. Thus, a relatively

Table III. Stress distribution in the 4 sutures

Suture	*Labiolingual arch (MPa)*	*Implant (MPa)*
Frontomaxillary	3.679-4.199	3.121-4.071
Zygomaticomaxillary	0.037-0.557	1.221-2.171
Temporozygomatic	0.557-1.078	5.021-5.971
Pterygopalatine	2.118-3.679	5.971-7.871

large protraction force of 800 g was loaded on both sides at a 20° to 30° angle with respect to the occlusal plane, depending on the position of the lower lip in both methods (Fig 6).

This model does not include the TMJ. The reason is that if the TMJ has been established, then the full temporozygomatic suture model cannot be established. Thus, obtaining accurate data on the displacement of the temporozygomatic suture is difficult. It conflicts with the focus of this study. Meanwhile, we loaded the boundary constraints at the top and rear of the condylar process. This approach can prevent unlimited rotation of the mandible under the loading force, simulating the action of the TMJ to a certain extent.

The y-axis represented sagittal displacement. The maxillary anterior teeth in the labiolingual arch model had labial movement of 0.142 mm, which was simply the difference between the forward displacement of those teeth and Point A. Point A of the maxilla moved 0.302 mm forward; the movement-effect ratio of the teeth to the maxilla was 0.47:1, which was close to the result of 0.58:1 in the labiolingual arch group obtained by Bao.[33] This indicated that our finite element analysis could reflect the movements of teeth and jaw caused by protraction in clinical practices. The small discrepancy might be because natural growth was allowed in their study, but it could not be assessed with finite element analysis in this study.

A tangent line was made from the protrusion of the outer margin of the condylar process, and the boundary constraints were imposed. The mandibular plane angle was obtuse. The mandibular condyle was located in the rear of the ascending ramus. Under the reaction force of protraction, the mandible underwent clockwise rotation, which led to backward displacement in the sagittal direction (along the y-axis).

In this study, the protraction point of the implant in the implant type of protraction model was between the root apices of the maxillary canines and first premolars. The site between the root apices of the maxillary lateral incisor and canine adopted by Ding et al[34] was not used because the root apices of the maxillary lateral incisor and canine have a thin bony wall. Furthermore, from the perspective of clinical practice of orthodontic treatment, the rubber band starting from the root apices of the maxillary lateral incisor and canine could easily press the upper lip and increase the patient's discomfort. The rubber band starting from the root apices of the maxillary canine and the first premolar was pulled out from both sides of the mouth. The thicker part of the upper lip was avoided to reduce the patient's discomfort. The protraction line was above the centers of resistance of the maxillary dental arch and the maxilla, and thus both the maxillary dental arch and the maxilla underwent clockwise rotation. An 800-g protraction force was imposed on the implant, the maxillary forward displacement was 0.275 mm, and the maxillary anterior teeth had a forward displacement of 0.164 mm. These results seemed contradictory because the maxilla and the maxillary dental arch were on the same curved surface, and the maxilla was posterior to the maxillary anterior teeth. The maxilla and the maxillary dental arch underwent clockwise rotation simultaneously, so the forward displacement of the maxilla was greater than that of the maxillary anterior teeth, and the maxillary anterior teeth did not undergo labial inclination. The patients selected by Ding et al were in the middle and late mixed dentition stages, and the protraction time was long. In addition to the displacement along the y-axis of the maxilla and the maxillary dental arch, the leveraging effect of the mandibular anterior teeth imposed on the maxillary anterior teeth after the establishment of shallow coverage and natural growth of the maxillary dental arch during the treatment of the crossbite also occurred. Therefore, the forward displacement of the maxillary anterior teeth was greater than that of the maxilla. Since the natural growth of the organism could not be shown by the 3D finite element method and the occlusion of the maxillary and mandibular anterior teeth was not modeled, the leveraging effect of the mandibular anterior teeth on the maxillary anterior teeth could not be simulated. The data obtained in this study simply indicated the displacement trend of maxillary protraction without tissue remodeling and occlusion. The downward displacements of the maxillary incisors and the maxilla were 0.312 and 0.253 mm, respectively; this further confirmed the clockwise rotation of the maxilla and the maxillary dental arch.

In this study, the displacement and stress nephogram showed that the forward displacement of the maxilla along the y-axis in the labiolingual arch model was 0.302 to 0.231 mm and closer to 0.302 mm. In the model with the implant, the nephogram of the forward displacement of the maxilla along the y-axis gradually decreased from the center of the protraction point to the periphery. The interval scale was 0.112, which was greater than that of the labiolingual arch model (0.071). Although the color of the nephogram of the

forward displacement of maxilla was at 0.275 mm, forward displacement of Point A was in the range of 0.387 to 0.275 mm and closer to 0.387 mm. The displacement along the y-axis of the maxilla caused by protraction using the implant was higher than that caused by the labiolingual arch.

The backward displacement (0.395 mm) of the mandible of the model with the implant was greater than that of the labiolingual arch model (0.124 mm). The stress distribution nephogram also showed that the stress of the former was greater than that of the latter. This might be because the higher protraction point increased the force arm and the moment on the maxilla, but the force arm of the mental region serving as anchorage was unchanged. Therefore, the stress and the backward displacement of the mandible were increased.

The displacement nephogram along the z-axis showed that the maxilla in the labiolingual arch model underwent upward displacement, which was consistent with the clinical cases. Because a tangent plane was made from the mandibular condyle and a boundary constraint was imposed, it was impossible to accurately show the mandibular displacement in the coronal direction along the z-axis. This problem is inevitable in building the physical model of the suture.

In this study, the protraction point of the labiolingual arch model was lower. The protraction line passed below the centers of resistance of the maxilla and the maxillary dental arch. Both the maxilla and the maxillary anterior teeth underwent upward displacement: ie, both underwent counterclockwise rotation. The protraction point of the model with the implant was higher than that in the labiolingual arch model. The protraction line passed over the centers of resistance of the maxilla and the maxillary dental arch. Both the maxilla and the maxillary anterior teeth underwent downward displacement: ie, both underwent clockwise rotation.

As shown in Table III, of the 4 sutures in the labiolingual arch model, the frontomaxillary suture had the most stress of 3.679 to 4.199 MPa. It had forward displacement of 0.160 mm along the y-axis and upward displacement of 0.205 mm along the z-axis. Its counterclockwise rotation was greater than that of other sutures. The displacement of the maxilla connected to it had a similar displacement. This might be due to the following reasons.

First, the frontomaxillary suture is on top of the maxilla and parallel to the cross-section of the maxilla. Furthermore, it has the smallest contact area with the frontal process. Second, the frontomaxillary suture is closer to the protraction point in the sagittal direction, and the bone surface in this region is smooth without the buffering effect of other sutures. Thus, the stress is little attenuated from the protraction point to the frontomaxillary suture, resulting in a greater displacement compared with the other sutures. Based on the displacement analysis, both the horizontal and vertical components of stress transmitted from the protraction point to the frontomaxillary suture were relatively high. The frontomaxillary suture plays a major role in maxillary protraction with the labiolingual arch.

The stress of the zygomaticomaxillary suture was 0.037 to 0.557 MPa, which was lower than that of other sutures. This might have been because the zygomaticomaxillary suture is located at the juncture of the maxilla and the zygoma, and the latter is an arcuated bone, leading to the reduction of stress transmitted to this region. The forward displacement along the y-axis of the maxilla connected to the zygomaticomaxillary suture was 0.160 mm. The upward displacement along the z-axis was 0.134 mm, which was close to the displacement of zygomaticomaxillary suture. However, the forward displacement of the zygomatic arch along the y-axis was 0.089 mm, and the upward displacement along the z-axis was 0.096 mm. These results indicated that the zygomaticomaxillary suture plays a role in the forward displacement of the maxilla and the zygoma in maxillary protraction and also influences the counterclockwise rotation of the maxilla. This might be because the zygomaticomaxillary suture is nearly parallel to the maxillary coronal plane. This is the reason for its major role in maxillary protraction with the labiolingual arch.

The stress of the temporozygomatic suture was as low as 0.557 to 1.078 MPa, which was greater than that of the zygomaticomaxillary suture. This might be because the temporozygomatic suture is close to the center of resistance of the maxilla. The rotation of the maxilla resulted in the stress concentration. Both its forward displacement along the y-axis (0.018 mm) and its downward displacement along the z-axis (0.018 mm) were smaller than those of the zygomaticomaxillary suture. The temporozygomatic suture did not change significantly in the maxillary protraction with the labiolingual arch. The forward displacement along the y-axis was small; this might have been because the temporozygomatic suture is located at the outermost margin of maxillofacial bone. The horizontal component of stress is buffered by the zygomaticomaxillary suture, and the stress is sharply reduced before being transmitted to the temporozygomatic suture. There was a downward displacement along the z-axis. However, the zygomatic bone anterior to the temporozygomatic suture and the maxilla underwent upward displacement, indicating that in protraction with the labiolingual arch the maxilla underwent counterclockwise rotation around the center

of resistance of the maxilla. Therefore, the temporozygomatic suture underwent downward displacement, whereas the frontomaxillary suture underwent upward displacement.

The stress of the pterygopalatine suture was as high as 2.118 to 3.679 MPa, which was similar to that of frontomaxillary suture. However, its forward displacement along the y-axis (0.018 mm) and downward displacement along the z-axis (0.018 mm) were lower than those of the frontomaxillary suture. When the maxilla underwent counterclockwise rotation, the maximum stress was located on the lower part of the pterygopalatine suture (Fig 12). The maxilla connected to the pterygopalatine suture underwent a large forward displacement. However, the displacement of the pterygopalatine suture was smaller (Fig 7). This was due to the relatively large sagittal distance from the protraction point to the pterygopalatine suture as well as the large variation of the deformation of the bones. The stress was buffered by the pterygopalatine suture, and the displacement was sharply reduced. Therefore, the pterygopalatine suture did not change significantly in maxillary protraction with the labiolingual arch.

The stress (3.121-4.071 MPa) and the forward displacement along the y-axis (0.051 mm) of the frontomaxillary suture in the model with the implant were not significantly different from those in the labiolingual arch model (Figs 7 and 8). However, the upward displacement of the frontomaxillary suture along the z-axis changed to downward displacement, resulting in clockwise rotation of the maxilla. Therefore, the frontomaxillary suture plays a major role in maxillary protraction with the implant.

The stress of the zygomaticomaxillary suture was 1.221 to 2.171 MPa, which was twice that of the labiolingual arch model. The forward displacement along the y-axis (0.275 mm) increased with the stresses (Fig 8). The upward displacement along the z-axis changed to downward displacement (Fig 10), which was 1 reason for the clockwise rotation of the maxilla. The stress of the zygomaticomaxillary suture in the implant model was still the lowest among all sutures. This was probably due to its specific position. However, the large displacement made the zygomaticomaxillary suture play a major role in maxillary protraction with the implant.

The stress of the temporozygomatic suture changed significantly in the range of 5.021 to 5.971 MPa. The stress was greater than that of the zygomaticomaxillary suture; this was because the temporozygomatic suture is closer to the center of resistance of the maxilla. The maxillary rotation caused stress concentration. The forward displacement along the y-axis (0.052 mm) was less significantly changed than that of the labiolingual arch model (Fig 8). Compared with the zygoma and the maxilla, the temporozygomatic suture showed a trend of upward displacement along the z-axis (Fig 10), indicating that the maxillary bones rotated around the center of resistance of the maxilla in a clockwise direction. The temporozygomatic suture underwent upward displacement, whereas the frontomaxillary suture underwent downward displacement.

The stress of the pterygopalatine suture was 5.971 to 7.871 MPa, which was twice that of the labiolingual arch protraction model. When the maxilla underwent clockwise rotation, the maximum stress was imposed on the upper part of the pterygopalatine suture (Fig 12). The forward displacement of the pterygopalatine suture along the y-axis (0.052 mm) increased with the stress but was still much smaller than the forward displacement of the maxilla along the y-axis (Fig 8). This was due to the large variation of deformation of the bones. The downward displacement along the z-axis changed little (0.018 mm). The pterygopalatine suture changed little in maxillary protraction with the implant.

A 16-year-old patient was chosen because she was a model without correction and treatment. Based on the characteristics of this subject, the model and analysis in this study demonstrate a certain universality and provide a significant guideline for clinical treatment.

This simulation study was conducted in the freeway space state because the mandibular molars do not contact. Therefore, the counterforces from the chin to the mandibular molar and from the mandibular molar to the maxillary molar were not considered.

In this study, we were unable to simulate the natural growth of bones and teeth, a common limitation of the finite element method. In addition, we could apply single loading and analyze the tendency of displacement and stress of the maxilla but could not obtain the nonlinear variations of displacement and stress in long-term loading. With these limitations, we aimed to provide a guide for clinical treatments instead of representing a clinical case.

CONCLUSIONS

A complete model of the maxillofacial bones including physical models of the sutures closely related to the growth of the maxilla was established using spiral CT combined with Mimics and ANSYS software.

1. After loading of the maxillary protraction model with the labiolingual arch, the maxilla underwent forward displacement, the maxillary anterior teeth underwent labial inclination, and the maxilla underwent counterclockwise rotation. These results were similar to the clinical findings, which suggested

the reasonability and feasibility of the modeling. The labiolingual arch is suitable for skeletal Class III patients with crossbite and deep overbite. The frontomaxillary and zygomaticomaxillary sutures played major roles in the forward displacement and counterclockwise rotation of the maxilla. The temporozygomatic and pterygopalatine sutures did not change significantly.

2. After loading of the maxillary protraction model with the implant, the maxilla underwent forward displacement. The maxillary anterior teeth did not undergo labial inclination, and the maxilla underwent clockwise rotation; these were consistent with the clinical findings. The implant type of protraction device is suitable for skeletal Class III patients with crossbite and open bite. Both the frontomaxillary and zygomaticomaxillary sutures played decisive roles in the forward displacement and clockwise rotation of the maxilla. The temporozygomatic and pterygopalatine sutures showed small changes.
3. According to the analyses of clinical cases and the data of this study, the labiolingual arch causes less stimulatory growth on the maxilla, whereas the implant causes greater stimulatory growth on the maxilla. Protraction with the labiolingual arch is more suitable for early skeletal Class III patients at younger ages; protraction with the implant was applicable to skeletal Class III patients in the late mixed dentition or early permanent dentition.

REFERENCES

1. Guyer EC, Ellis EE 3rd, McNamara JA Jr, Behrents RG. Components of class III malocclusion in juveniles and adolescents. Angle Orthod 1986;56:7-30.
2. Kapust AJ, Sinclair PM, Turley PK. Cephalometric effects of face mask/expansion therapy in Class III children: a comparison of three age groups. Am J Orthod Dentofacial Orthop 1998;133:204-12.
3. Spalj S, Mestrovic S, Lapter Varga M, Slaj M. Skeletal components of class III malocclusions and compensation mechanisms. J Oral Rehabil 2008;35:629-37.
4. Gallagher RW, Miranda F, Buschang PH. Maxillary protraction: treatment and posttreatment effects. Am J Orthod Dentofacial Orthop 1998;113:612-9.
5. da Silva Filho OG, Magro AC, Capelozza Filho L. Early treatment of the Class III malocclusion with rapid maxillary expansion and maxillary protraction. Am J Orthod Dentofacial Orthop 1998; 113:196-203.
6. Saadia M, Torres E. Sagittal changes after maxillary protraction with expansion in class III patients in the primary, mixed, and late mixed dentitions: a longitudinal retrospective study. Am J Orthod Dentofacial Orthop 2000;117:669-80.
7. Vaughn GA, Mason B, Moon HB, Turley PK. The effects of maxillary protraction therapy with or without rapid palatal expansion: a prospective, randomized clinical trial. Am J Orthod Dentofacial Orthop 2005;128:299-309.
8. Major MP, Wong JK, Saltaji H, Major PW, Flores-Mir C. Skeletal anchored maxillary protraction for midface deficiency in children and early adolescents with Class III malocclusion. JWFO 2012;1: e47-54.
9. Nguyen T, Cevidanes L, Cornelis MA, Heymann G, de Paula LK, De Clerck H. Three-dimensional assessment of maxillary changes associated with bone anchored maxillary protraction. Am J Orthod Dentofacial Orthop 2011;140:790-8.
10. Sun Z, Hueni S, Tee BC, Kim H. Mechanical strain at alveolar bone and circummaxillary sutures during acute rapid palatal expansion. Am J Orthod Dentofacial Orthop 2011;139:e219-28.
11. Smalley WM, Shapiro PA, Hohl TH, Kokich VG, Brånemark PI. Osseointegrated titanium implants for maxillofacial protraction in monkeys. Am J Orthod Dentofacial Orthop 1988;94: 285-95.
12. Lee H, Ting K, Nelson M, Sun N, Sung SJ. Maxillary expansion in customized finite element method models. Am J Orthod Dentofacial Orthop 2009;136:367-74.
13. Gautam P, Valiathan A, Adhikari R. Maxillary protraction with and without maxillary expansion: a finite element analysis of sutural stresses. Am J Orthod Dentofacial Orthop 2009;136:361-6.
14. Gautam P, Valiathan A, Adhikari R. Stress and displacement patterns in the craniofacial skeleton with rapid maxillary expansion: a finite element method study. Am J Orthod Dentofacial Orthop 2007;132:e1-11.
15. Yu HS, Baik HS, Sung SJ, Kim KD, Cho YS. Three-dimensional finite-element analysis of maxillary protraction with and without rapid palatal expansion. Eur J Orthod 2007;29:118-25.
16. Mao JJ. Mechanobiology of craniofacial sutures. J Dent Res 2002; 81:810-6.
17. Iseri H, Tekkaya AE, Oztan O. Bilgiç. Biomechanical effects of rapid maxillary expansion on the craniofacial skeleton, studied by the finite element method. Eur J Orthod 1998;20:347-56.
18. Verrue V, Dermaut L, Verhegghe B. Three-dimensional finite element modelling of a dog skull for the simulation of initial orthopaedic displacements. Eur J Orthod 2001;23:517-27.
19. Jafari A, Shetty KS, Kumar M. Study of stress distribution and displacement of various craniofacial structures following application of transverse orthopedic forces—a three-dimensional FEM study. Angle Orthod 2003;73:12-20.
20. Nanda R, Goldin B. Biomechanical approaches to the study of the alterations of facial morphology. Am J Orthod 1980;78:213-26.
21. Song RY, Liu CM. Cleft lip and palate repair. 4th ed. Beijing, China: People's Medical Publishing House; 2003.
22. Brandt HC, Shapiro PA, Kokich VG. Experimental and postexperimental effects of posteriorly directed extraoral traction in adult Macaca fascicularis. Am J Orthod 1979;75:301-17.
23. Chabanas M, Luboz V, Payan Y. Patient specific finite element model of the face soft tissues for computer-assisted maxillofacial surgery. Med Image Anal 2003;7:131-51.
24. Hampson D. Facial injury: a review of biomechanical studies and test procedures for facial injury assessment. J Biomech 2000;30: 1-7.
25. Ngan P, Wei SH, Hägg U, Yiu CK, Merwin D, Stickel B. Effect of protraction headgear on Class III malocclusion. Quintessence Int 1992;23:197-207.
26. Cozzani G. Extraoral traction and class III treatment. Am J Orthod 1981;80:638-50.
27. Hickham JH. Maxillary protraction therapy: diagnosis and treatment. J Clin Orthod 1991;25:102-13.
28. Itoh T, Chaconas SJ, Caputo A, Matyas J. Photoelastic effects of maxillary protraction on the craniofacial complex. Am J Orthod 1985;88:117-24.

29. Hata S, Itoh T, Nakagawa M, Kamogashira K, Ichikawa K, Matsumoto M, et al. Biomechanical effects of maxillary protraction on the craniofacial complex. Am J Orthod Dentofacial Orthop 1987;91:305-11.
30. Billiet T, de Pauw G, Dermaut L. Location of the centre of resistance of the upper dentition and the nasomaxillary complex. An experimental study. Eur J Orthod 2001;23: 263-73.
31. Zeng XL. Contemporary orthodontics clinic manual. 1st ed. Beijing, China: Peking Medical University Press; 2000.
32. Gautam P, Valiathan A, Adhikari R. Skeletal response to maxillary protraction with and without maxillary expansion: a finite element study. Am J Orthod Dentofacial Orthop 2009;135:723-8.
33. Bao YJ. Comparison with the effect of the skeletal-dental and soft tissue profile changes of maxillary protraction with labiolingual appliances or rapid maxillary expansion appliances [dissertation]. Changchun, Jilin, China: Jilin University; 2009.
34. Ding P, Zhou YH, Lin Y, Qiu LX. Miniplate implant anchorage for maxillary protraction in Class III malocclusion. Chin J Stomatol 2007;42:263-7.